Yonsei Medical Journal
Vol. 41, No. 1, pp. 8−16, 2000

☐ Original Article ☐

Primary Malignant Rhabdoid Tumor of the Brain: CT and MR Findings

Choon-Sik Yoon[1], Sylvester Chuang[2], and Venita Jay[3]

Abstract

Purpose: To describe the CT and MR findings of primary malignant rhabdoid tumor (MRT) of the brain, which is a rare but very aggressive neoplasm in childhood. **Materials and Methods:** Retrospectively, we evaluated the CT and MR findings of 5 patients of primary MRT of the brain with a review of clinical records. **Results:** The primary MRTs of the brain were large (n=4) with a tendency to be associated with necrosis, hemorrhage (n=2) and calcification (n=2). Solid components of the tumor showed increased attenuation on precontrast CT scan and iso- or slightly hyper-signal intensity on T2-weighted images probably due to hypercellularity. Solid components of the tumor were also well enhanced on contrast-enhanced CT scan (n=5) and MRI (n=2). In 1 case with intratumoral bleeding, MR findings were variable on T1-weighted and T2-weighted images. Intracranial and intraspinal metastasis were found in 2 cases on preoperative MR studies. Follow-up CT and MR studies showed recurrence of the tumor and/or leptomeningeal metastasis in 3 cases. **Conclusions:** Although CT and MR findings of primary MRT of the brain are nonspecific, a tendency toward large size, calcification and intratumoral bleeding may be attributed to CT and MR findings. The solid components of tumors could present hyperdense on precontrast CT scan and iso- or slightly hyper-signal intensity on T2-weighted MR image. Preoperative and follow-up MR studies are important to detect metastatic foci.

Key Words: Brain, neoplasms, CT brain neoplasms, MR

INTRODUCTION

First described in 1978,[1] malignant rhabdoid tumor (MRT) is recognized as one of the most malignant tumors of the kidney. Although MRTs were originally and most frequently reported as arising in the kidney,[2-6] similar neoplasms have been reported in the thymus,[7] liver[8] and various soft-tissue sites.[8-10] To our knowledge, primary MRT in the brain is extremely rare, with fewer than 100 reported cases to date.[11-20] Only some of these reports have included a description of the imaging findings.[15-20] In this report, we describe CT and MR findings in 5 cases of intracranial MRT and review radiological findings of previously reported cases.

Received February 26, 1999
Accepted November 15, 1999

[1]Department of Diagnostic Radiology, Research Institute of Radiological Science, Yonsei University College of Medicine, Seoul, Korea, [2]Division of Pediatric Neuroradiology, Department of Diagnostic Imaging, [3]Division of Neuropathology, Department of Pathology, The Hospital for Sick Children, University of Toronto, Toronto, Canada.

Address reprint request to Dr. C. S. Yoon, Department of Diagnostic Radiology, Yongdong Severance Hospital, Yonsei University College of Medicine, Yongdong P.O. Box 1217, Seoul 135-270, Korea. Tel: 82-2-3497-3514, Fax: 82-2-3462-5472, E-mail: yooncs58@yumc.yonsei.ac.kr

MATERIALS AND METHODS

We retrospectively evaluated 5 patients with primary MRT of the brain including 1 previously reported (case 1). All 5 patients underwent preoperative brain CT scans before and after intravenous injection of 2 ml/kg of non-ionic contrast agents with slice thickness of 5−10 mm. Two patients underwent MR studies with a Magnetom 1.5 T (Siemens medical System, Enlangen, Germany) with head coil. The unenhanced T1-weighted images (TR/TE, 520−608/10 msec) and T2-weighted images (TR/TE, 2800−3000/90−120 msec) were obtained, and then contrast-enhanced T1-weighted images (TR/TE, 680/22 msec) after intravenous injection of 0.1 mmol/kg of gadopentetate dimeglumine (Magnevist; Schering, Berlin, Germany) were acquired. The matrix size was 144−180×256, and various fields of view were applied according to the patients size, ranging from 20 to 25 cm. The slice thickness was 5 mm with 2.5 mm interslice gap. Our 5 patients were comprised of 2 girls aged 49 and 71 months and 3 boys aged 9

and 14 months and 15 years. The diagnosis of MRT was established by pathology following surgical resection. Abdominal CT scans also were obtained postoperatively in 4 patients to rule out renal neoplasm except for 1 case which was associated with rapid deterioration of clinical course after surgery. Pathologic investigations included light microscopic examination, immunohistochemistry and electron microscopy. Immunohistochemical studies were performed by the immunoperoxidase technique using a variety of markers including glial fibrillary acidic protein (GFAP, polyclonal, 1 : 200. Dako, Glostrup, Denmark), synaptophysin (monoclonal, 1 : 5, Sternberger-Meyer Immunocytochemicals Inc., Baltimore, MD, USA), neuron specific enolase (NSE, polyclonal, 1 : 250, Dako, Glostrup, Denmark), epithelial membrane antigen (EMA, monoclonal, 1 : 10, Dako, Glostrup, Denmark), low molecular weight cytokeratin (CEA, polyclonal, 1 : 200, Dako, Glostrup, Denmark), S-100 protein (polyclonal, 1 : 200, Dako, Glostrup, Denmark), vimentin (monoclonal, 1 : 300, Sigma, St. Louis, MO, USA), and desmin (monoclonal, 1 : 20, Dako, Glostrup, Denmark). For electron microscopy, tissue was fixed in the universal fixative (equal parts of 4% formaldehyde and 1% glutaraldehyde) and post-fixed in 1% Osmium tetroxide, dehydrated in graded alcohols and prophylene oxide and embedded in epon. One micrometer-thick sections were stained

Table 1. Summary of Clinical Findings in 5 Cases of Primary Malignant Rhabdoid Tumor of the Brain

Case No.	Age	Sex	Symptoms	Treatment	Outcome
1.	9 m	M	vomiting, irritability	partial resection, chemotherapy	died 4 months after op.
2.	15 y	M	headache, vomiting	total resection, chemotherapy, RT	alive 6 months after op.
3.	14 m	M	macrocephaly	biopsy	discharge 1 month after op. with 'DNR' state
4.	4 y	F	headache, vomiting, seizure	total resection, chemotherapy, RT	alive after 3 months after op.
5.	6 y	F	headache, left 7^{th} nerve palsy	debulking excision, chemotherapy, RT	alive 13 months after op.

op., operation; RT, radiation therapy; 'DNR', 'do not resuscitate'.

Table 2. Summary of CT and MR Findings in 5 Cases of Primary Malignant Rhabdoid Tumor of the Brain

Case No.	Size (cm)	Location	Pre-contrast	CT post-contrast enhanced pattern	T1WI pre/Gd	MR T2WI	T1WI post/Gd	Calc.	Edema	Necro-sis	Hemo-rrhage	Intraspinal metastasis	F/U CT/MR
1.	2.7×2.8×4	pineal	high	diffuse		N/A		none	none	none	+	−	recurrence
2.	6×7×3.5	Rt.F	mixed	patchy		N/A		fleck	mild	multiple	−	−	no recurrence
3.	9×7.8×9	Lt.FTP	mixed	patchy	mixed	mixed	peripheral patchy	none	mod.	multiple	+	preop.	recurrence progression of metastatic lesion
4.	5.5×4.9×6	Lt.T	high	diffuse		N/A		Dense	mod.	multiple	−	postop.	Recurrence leptomeningeal spread
5.	1×1.7×1.3 multifocal	vermis	high inhomogeneous	diffuse	low	iso	diffuse	none leptomeningeal spread	none	none	−	preop.*	Initial improvement

Calc., calcification; T1WI, T1-weighted image; T2WI, T2-weighted image; preop., preoperative; postop., postoperative; F/U, follow up; N/A, not available; F, frontal lobe; FTP, frontotemporoparietal lobe; T, temporal lobe; cbll, cerebellum; Ref., Reference; Rt., right; Lt., left; mod., moderate.

* also include left cerebellopontine metastatic nodule.

Table 3. Summary of Clinical Findings and Outcome in Previously Reported Cases in the Literature

Case No.	Age	Sex	Symptoms	Treatment	Outcome
Reference 15	3 y	F	lethargy, neck pain, vomiting	partial resection, chemotherapy, RT	alive 5 months after op.
Reference 16	4 y	M	headache	partial resection, RT	died 1 month following presentation
Reference 17	25 m	F	lethargy, ataxia, vomiting	partial resection, chemotherapy, RT	died 6 months after op.
	8 m	M	lethargy, irritability, vomiting	total resection, chemotherapy, RT	died 15 months after op.
	66 m	F	diplopia, fatigue	total resection, chemotherapy, RT	died 6 months after op.
Reference 19	33 m	M	lethargy, vomiting, ataxia	total resection, chemotherapy, RT	died 8 months after op.
Reference 20	2 y	M	weight loss, vomiting	subtotal resection, chemotherapy, RT	died 7.5 months after op.
Reference 27	18 m	F	loss of balance, irritability	subtotal resection, chemotherapy, RT	died 5.5 months after op.
	5 y	M	lethargy, neck pain, irritability	biopsy, RT	died 15 days after op.

RT, radiation therapy; op., operation.

Fig. 1. *Case 2: A 15-year-old boy with right frontal primary MRT. (A) Precontrast CT scan shows a mixed density large tumor with moderate edema in the right frontal lobe. (B) Postcontrast enhanced CT scan shows patchy enhancing tumor. Areas of low density are suggestive of necrosis.*

with toluidine blue. Ultrathin sections were examined under a Phillips 400 transmission electron microscope.

RESULTS

Details of symptoms and clinical course are summarized in Table 1. Clinical symptoms were variable in each case. The tumors were large, except for case 5. MRT occurred mostly in early childhood, less than 6 years of age in 4 cases but 1 patient (case 5) was 15 years old. CT and MR findings are summarized in Table 2. We also summarized previously reported cases in Table 3 and 4. Solid components of MRT except the necrotic area showed increased attenuation compared to normal gray matter in precontrast CT scan in all cases (Fig. 1A, 2A, and 3A), which were well enhanced after contrast administration (Fig. 1B, 2B, and 3B). Calcifications were seen in 2 cases (case 2 and case 4) (Fig. 3A). In case 3, marked tumor necrosis and severe hemorrhage were observed on MR images with iso- to high signal intensity on T1-weighted image and decreased to iso-signal intensity on T2-weighted images (Fig. 2, C and D). In case 5, CT scan showed a small lobulated enhancing mass located in the midline posterior fossa (Fig. 4A), but

Table 4. Summary of CT and MR Findings in Previously Reported Cases in the Literature

Case No.	Size (cm)	Location	CT			MR			Calc.	Edema	Necrosis	Hemorrhage	Intraspinal metastasis	F/U CT/MR leptomeningeal spread
			precontrast	postcontrast enhanced pattern		T1WI pre/Gd	T2WI	T1WI post/Gd						
Ref. 15	large	Lt. cbll	mixed	intense			N/A							
Ref. 16	N/A	multifocal	high	intense			N/A		linear, punctate					
Ref. 17	6×5×5.5	Lt. P	mixed	patchy			N/A		none	severe	multiple			recurrence, frontal
	6×5×6	Lt. frontal horn (intraventricular)	slightly high	diffuse			N/A		few flecks	none	multiple			recurrence, cerebellopontine
	5.5×5×5	Lt. trigone	N/A	N/A		iso	iso	patchy	N/A	mod.	multiple			recurrence, cerebellar and (intraventricular) cerebellopontine
Ref. 19	large	Lt. F	N/A	inhomogeneous		N/A			mod.	multiple				subarachnoid dissemination
Ref. 20	N/A	vermis	high	diffuse		low	iso	diffuse	none	N/A	multiple			recurrence
Ref. 27	N/A	vermis	mixed	enhanced			N/A		N/A	N/A	N/A			hydrocephalus
	N/A	vermis multifocal	high	N/A			N/A		N/A	N/A	N/A	+		N/A.

Calc., calcification; T1WI, T1-weighted image; T2WI, T2-weighted image; preop., preoperative; F/U, follow up; N/A, not available; F, frontal lobe; P, parietal lobe; cbll, cerebellum; Ref., Reference; Rt., right; Lt., left; mod., moderate.

MR study showed a small low- to iso-intense tumor arising from cerebellar vermis on T1-weighted images and isointense on T2-weighted images with diffuse and somewhat inhomogeneous enhancement after contrast administration (Fig. 4, B, C and D). In case 3 and case 5, preoperative MR studies detected metastatic tumors in the intraspinal subarachnoid space and left cerebellopontine subarachnoid space (Fig. 4E). Postoperative abdominal CT scans showed no definite renal masess in 4 cases. Follow-up CT and MR studies showed tumor recurrence or residual tumor growth (cases 1, 3, 4) and leptomeningeal metastasis (cases 3 and 4). Follow-up CT and MR studies of the remaining 2 cases showed no residual or recurrent tumor (case 2) and no metastatic lesion with the disappearance of preexisting metastatic lesions following chemotherapy and radiation (case 5). The clinical outcome of our cases was poor except for case 2 and case 5. Case 1 died 4 months after operation and case 3 was discharged 1 month after operation with rapid deterioration of clinical state. Case 4 showed progression of leptomeningeal metastasis despite intensive chemotherapy and radiation therapy following operation. Case 5 is still alive 13 months after operation.

Pathologic examination revealed the characteristic features of MRT with prominent nucleoli, high mitotic index, tumor necrosis and cytoplasmic globular inclusions in tumor cells which were immunopositive for vimentin (Fig. 5A) and cytokeratin (Fig. 5B). The tumors showed variable positivity for cytokeratin and epithelial membrane antigen, and S-100, while they showed negative for desmin, GFAP, synaptophysin and neurofilaments. By electron microscopy, perinuclear filamentous whorls comprised of bundles of intermediate filaments were identified in every case, confirming the pathologic diagnosis of MRT.

DISCUSSION

MRT is a highly aggressive malignant neoplasm originally described as a sarcomatous variant of Wilms' tumor with a poor prognosis. The term 'rhabdoid' originated from the light microscopic similarity to rhabdomyosarcoma, but a myogenous origin has been ruled out on the basis of the subsequently observed ultrastructural and immunohistochemical features.[14]

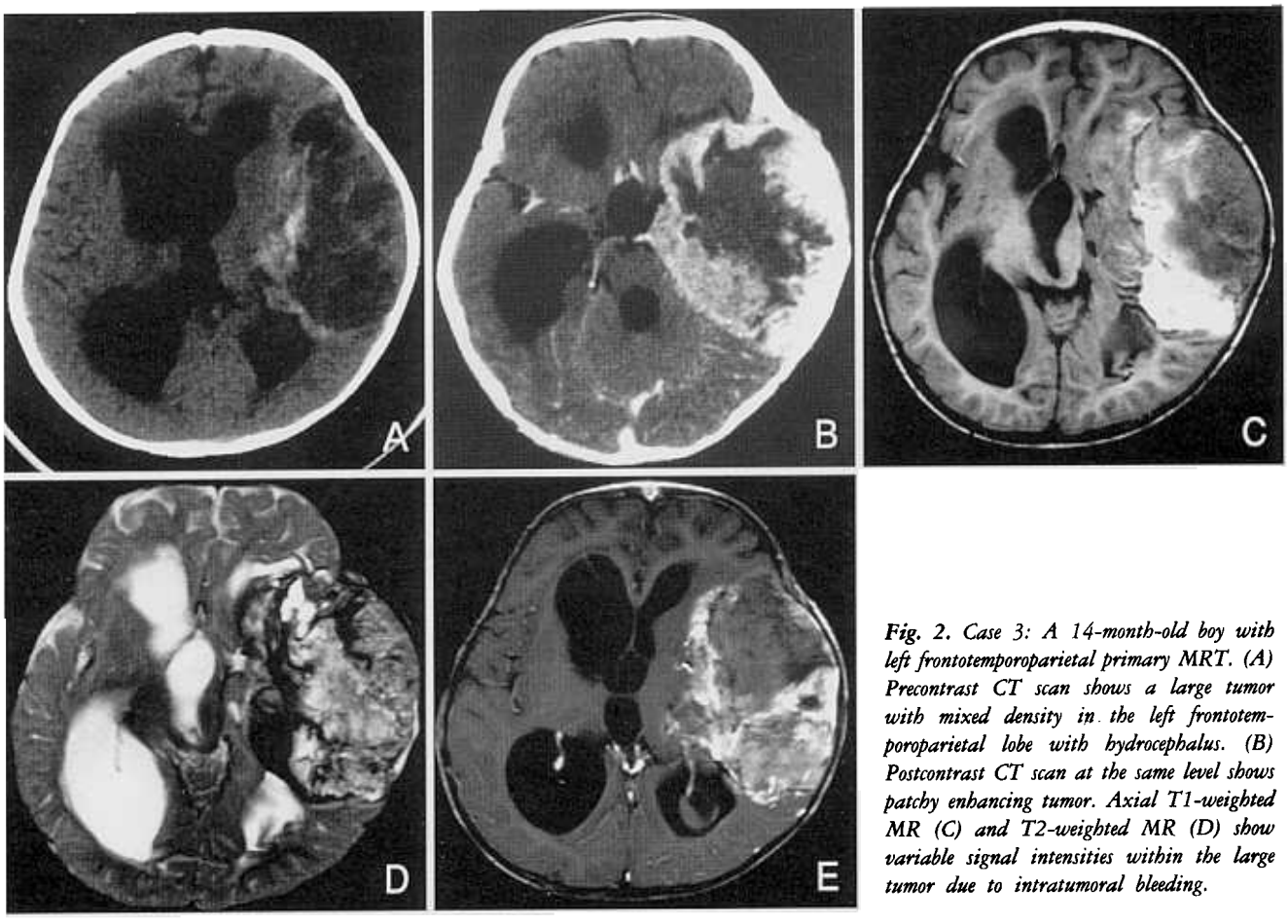

Fig. 2. Case 3: A 14-month-old boy with left frontotemporoparietal primary MRT. (A) Precontrast CT scan shows a large tumor with mixed density in the left frontotemporoparietal lobe with hydrocephalus. (B) Postcontrast CT scan at the same level shows patchy enhancing tumor. Axial T1-weighted MR (C) and T2-weighted MR (D) show variable signal intensities within the large tumor due to intratumoral bleeding.

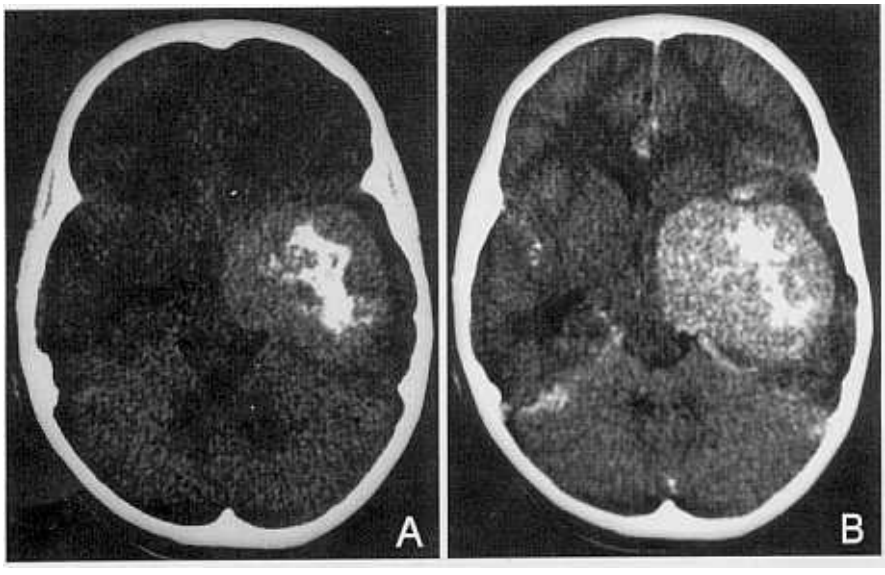

Fig. 3. Case 4: A 4-year-old girl with left temporal primary MRT. (A) Precontrast CT scan shows a large hyperdense mass with dense calcifications arising from the left temporal lobe. (B) Postcontrast CT scan shows a diffuse enhancing mass.

The renal tumor usually occurs in early childhood with a peak incidence at 13–16 months.[21,22] Bonin et al. reported the coexistence of renal MRT with cerebellar medulloblastoma, pineoblastoma, cerebral

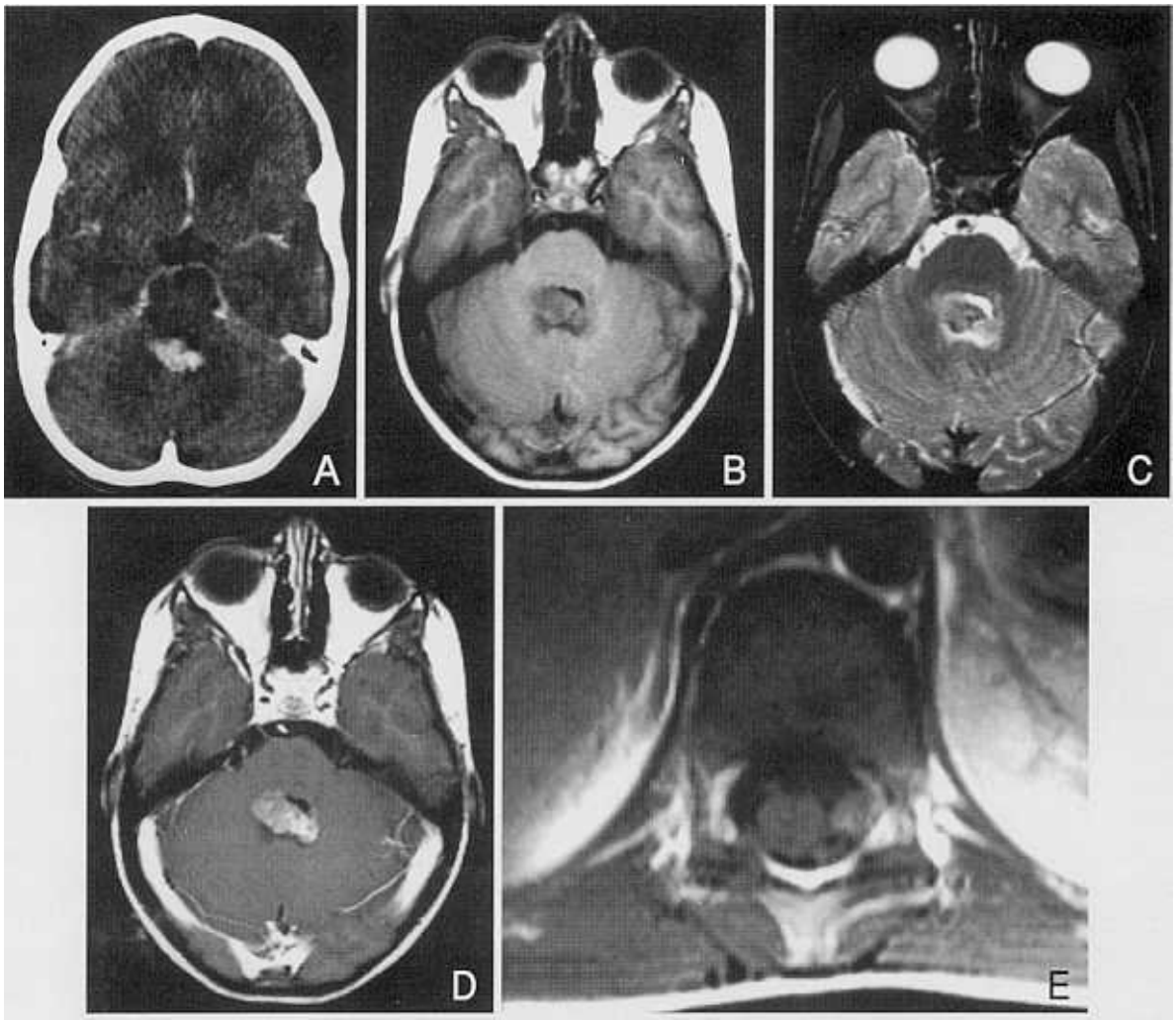

Fig. 4. Case 5: A 6-year-old girl with posterior fossa primary MRT. (A) Postcontrast axial CT scan shows a small lobulated well-enhanced mass located in the 4th ventricle. Axial T1-weighted MR (B), and axial T2-weighted MR (C) show a slightly low- to isointense mass relative to gray matter arising from the fourth ventricle area. Postcontrast axial T1-weighted MR (D), and postcontrast axial T1-weighted spine MR (E) obtained at the level of T11-T12 show relatively homogeneous enhancing mass at the primary site and focal enhancing nodule in the left intradural and extramedullary space at the T11-T12 level suggesting metastatic lesion.

primitive neuroectodermal tumor, and malignant subependymal giant cell astrocytoma.[23] A case of concomitant renal and presumed primary brain MRT has also been described.[23] The CNS MRT can ocurr in the fourth ventricle.[24] Brain metastases from renal MRT may also occur and tend to favor the cerebrum and may be multiple.[20] Due to similar pathologic features, it may be difficult to distinguish between primary CNS MRT and metastases from a renal primary MRT in cases of coexistent renal and brain MRT.[24,25] Our 4 cases with postoperative abdominal CT scan had no renal tumor, but the abdominal CT scan was not available in case 3.

Previous reports of primary MRT of the brain have usually shown a large tumor at the time of diagnosis with variable symptoms such as headache, lethargy, irritability and vomiting.[18,20] Our cases also showed large tumors and similar clinical symptoms except for case 5, which presented as a small tumor arising from cerebellar vermis with left facial weakness due to metastatic lesion to the left cerebellopontine angle area. Caldemyer et al. described that 9 of 11 known cases of primary central nervous system MRT occurred in cerebellum alone or in combination with a

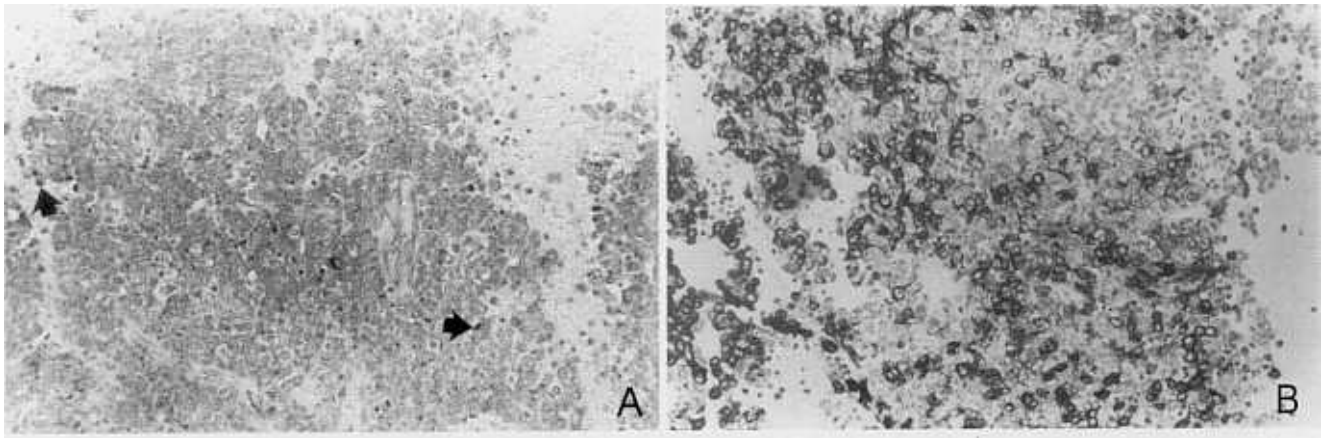

Fig. 5. (A) MRT with vimentin-positive globular inclusions in the cytoplasm of the tumor cell (arrows). The tumor shows large nuclei with prominent nucleoli and mitotic figures. Immunoperoxidase stain for vimentin, ×280. (B) Prominent cytokeratin immunoreactivity in the cytoplasm of tumor cells in the same case as illustrated in figure 5 (A). Immunoperoxidase stain for low molecular weight cytokeratin, ×280.

supratentorial tumor.[20] But Hanna et al. described 3 cases arising from the left cerebral hemisphere with 2 cases of intraventricular origin.[18] Our cases occurred in variable locations including the pineal region (case 1), supratentorial region (cases 2, 3, 4) and cerebellar vermis with intraventricular extension (case 5).

Primary MRTs of the brain have been reported from newborns up to 13 years of age, with the highest incidence of MRT in the first 2 years of life.[11,12,14,18,24,26,27] Ages of 4 of our cases were less than 6 years, similar to that of previously reported cases,[11,14,16,18] but one case was 15 years old.

Hanna et al. described that although the preoperative imaging findings described were nonspecific, there was some consistency among their cases such as large tumor size, multiple necrotic or cystic foci, a patchy pattern of enhancement on CT and MR studies and association with moderate to marked adjacent parenchymal edema.[18] In our cases, preoperative enhanced CT scans showed hyperdense solid components of tumors with or without necrotic foci. Hyperdense tumors enhanced well after contrast administration. The hyperdense solid component represented the hypercellular portion of the tumor by microscopic study and pathologic correlation. Low density areas of tumor without enhancement were necrotic areas by histology. Intratumoral calcification has been described in 3 of 14 reported cases. In our cases, parenchymal edema due to tumor was variable, ranging from none to a moderate degree, similar to another report.[18]

Because the most common site of MRT in the brain is the posterior fossa,[13] differential diagnosis must include medulloblastoma and ependymoma.[11,18,20,27] Age at onset of MRT is younger than in medulloblastoma, and size of MRT is larger than that of medulloblastoma.[11] CT and MRI may show polymorphic zones in MRT and more homogeneous in medulloblastoma.[11]

MR findings of primary MRT of the brain have been very limited.[11,18,20] Tumors were hypo- or isointense on T1-weighted image and iso- or hyperintense on T2-weighted image relative to the gray matter.[11,18,20] In our cases, case 5 showed relatively homogeneous signal characteristics on T1- and T2-weighted images, but case 3 showed mixed signal intensity on T1-and T2-weighted images due to extensive necrosis and intratumoral hemorrhage. Our 2 cases with intratumoral hemorrhage (cases 1, 3) had very poor clinical outcomes similar to the previously reported case with tumor hemorrhage.[27] Tumors in case 1 and case 3 were very vascular as confirmed by surgery and pathology.

Postoperative follow-up CT and MR studies have invariably shown tumor recurrence at the primary site and tumor spread to the subarachnoid space or meninges[18,20] suggesting an aggressive clinical course. Even preoperative CT or MR studies[16] have demonstrated multiple metastatic foci as in our case 3 and case 5.

Prognosis for reported cases has been generally poor.[18,20] Survival of all reported cases was less than 8 months except for one case, who died 15 months after initial diagnosis even though surgery, chemo-

therapy and radiation therapy were given.[17-20] In our cases, case 1 died 4 months after operation and postoperative chemotherapy with carboplatinum, ifosphamide and etoposide and case 3 had a poor clinical outcome after operation due to tumoral bleeding. The 3 remaining cases are still alive after surgery and postoperative chemotherapy with iphosphamide, Vp-16 and carboplatinum, and radiation therapy. Case 5 is alive more than 13 months after surgery.

The histogenesis of MRT is underdetermined. MRT is characterized by light microscopic features that include a diffuse growth pattern of predominantly polygonal cells, vesicular nuclei with prominent nucleoli, and scattered cells that contain a cytoplasmic hyaline globular inclusion adjacent to the nucleus.[14] MRTs show immunohistochemical positivity for vimentin and epithelial markers such as epithelial membrane antigen and cytokeratin[14,18,24,27] as demonstrated in all our cases. Unlike rhabdomyosarcoma, immunoreactions for myoglobin, desmin or myosin are negative.[4,10,14,20] Immunohistochemically, MRTs are also negative when stained with antisera to synaptophysin, S-100, neuron-specific enolase, and neurofilaments in contradistinction to primitive neuroectodermal tumors.[27] Electron microscopy demonstrates intracytoplasmic whorling filaments that represent vimentin.[17,22,27]

In summary, although CT and MR findings of primary MRT of the brain are nonspecific, a tendency toward large size, calcification and intratumoral bleeding may be attributed to CT and MR findings. The solid components of MRT, presenting hyperdense on precontrast CT and iso- or slightly hyper-signal intensity on T2-weighted MR image due to hypercellularity, are well enhanced after contrast administration. Preoperative and follow-up MR studies of the brain and spine with contrast enhancement are necessary for evaluation of the primary site as well as metastatic foci.

REFERENCES

1. Beckwith JB, Palmer NF. Histopathology and prognosis of Wilms' tumor: results from the First national Wilms' tumor study. Cancer 1978;41:1937-48.
2. Haas JE, Palmer NF, Weiberg AG, Beckwith JB. Ultrastructure of malignant rhabdoid tumor of the kidney. A distinctive renal tumor of children. Hum Pathol 1981; 12:646-57.
3. Fung CHK, Gonzalez-Crussi F, Yonan TM, Martinez N. 'Rhabdoid' Wilms' tumor: an ultrastructural study. Arch Pathol Lab Med 1981;105:521-3.
4. Schmidt D, Harms D, Zieger G. Malignant rhabdoid tumor of the kidney. Histopathology, ultrasturcture and comments on differential diagnosis. Virchows Arch (A) 1982;398:101-8.
5. Rousseau-Merck M-F, Nogues C, Nezelof C, Marin-Cudraz B, Paulin D. Infantile renal tumors associated with hypercalcemia: characterization of intermediate-filament clusters. Arch Pathol Lab Med 1983;107:311-4.
6. Vogel AM, Gown AM, Caughlan J, Haas JE, Beckwith JB. Rhabdoid tumors of the kidney contain mesenchymal-specific and epithelial-specific intermediate filament proteins. Lab Invest 1984;50:232-8.
7. Lemos LB, Hamoudi AB. Malignant thymic tumor in an infant (malignant histiocytoma). Arch Pathol Lab Med 1978;102:84-9.
8. Gonzalez-Crussi F, Goldschmidt RA, Hsueh W, Trujillo YP. Infantile sarcoma with intracytoplasmic filamentous inclusions: distinctive tumor of possible histiocytic origin. Cancer 1982;49:2365-75.
9. Lynch HT, Shurin SB, Dahms BB, Izant RJ Jr, Lynch J, Danes BS. Paravertebral malignant rhabdoid tumor in infancy: in vitro studies of a familial tumor. Cancer 1983; 52:290-6.
10. Tsuneyoshi M, Daimaru T, Hashimoto H, Enjoji M. Malignant soft tissue neoplasms with the histologic features of renal rhabdoid tumors: an ultrastructural and immunohistochemical study. Hum Pathol 198516:1235-42.
11. Martnez-Lage JF, Nieto A, Sola J, Domingo R, Costa TR, Poza M. Primary malignant rhabdoid tumor of the cerebellum. Child's Nerv Syst 1997;13:418-21.
12. Sotelo-Avila C, Gonzalez-Crussi F, deMello D, Vogler C, Gooch WM, Gale G, et al. Renal and extrarenal rhabdoid tumors in children: a clinicopathologic study of 14 patients. Semin Diagn Pathol 1986;3:151-63.
13. Rorke LB, Packer RJ, Biegel JA. Central nervous system atypical teratoid/rhabdoid tumors of the infancy and childhood: definition of an entity. J Neurosurg 1996;85:56-65.
14. Biggs PJ, Garen PD, Pawers JM, Garvin AJ. Malignant rhabdoid tumor of the central nervous system. Hum Pathol 1987;18:332-7.
15. Jakate SM, Marsden HB, Ingram L. Primary rhabdoid tumor of the brain. Virchows Arch (A) 1988;4:393-7.
16. Ho PSP, Lee WH, Chen CY, Chou TY, Wang YC, Sun MJ, et al. Primary malignant rhabdoid tumor of the brain: CT characteristics. J Comput Assist Tomogr 1990;14: 461-3.
17. Argonovich AL, Ang LC, Griebel RW, Kobrinsky NL, Lowry N, Tchang SP. Malignant rhabdoid tumor of the central nervous system with subarachnoid dissemination. Surg Neurol 1992;37:410-4.
18. Hanna SL, Langston JW, Parham DM, Douglass EC. Primary malignant rhabdoid tumor of the brain: clinical, imaging, and pathologic findings. Am J Neuroradiol 1994; 14:107-15.

19. Muller M, Hubbard SL, Provias J, Greenberg M, Becker LE, Rutka JT. Malignant rhabdoid tumour of the pineal region. Can J Neurol Sci 1994;21:273-7.
20. Caldemyer KS, Smith RR, Azzarelli B, Boaz JC. Primary central nervous system malignant rhabdoid tumor: CT and MR appearance simulates a primitive neuroectodermal tumor. Pediatr Neurosurg 1994;21:232-6.
21. Chang C, Ramirez N, Sakr WA. Primitive neuroectodermal tumor of the brain associated with malignant rhabdoid tumor of the liver. Pediatr Pathol 1989;9:307-19.
22. Sisler CL, Siegel MJ. Malignant rhabdoid tumor of the kidney: radiologic features. Radiology 1989;172:211-2.
23. Bonin JM, Rubinstein LJ, Palmer NF, Beckwith JB. The association of embryonal tumors originating in the kidney and in the brain. A report of seven cases. Cancer 1984; 54:2137-46.
24. Biegel JA, Rorke LB, Packer RJ, Emanuel BS. Monosomy 22 in rhabdoid or atypical tumors of the brain. J Neurosurg 1990;73:710-4.
25. Weeks DA, Beckwith JB, Mierau GW, Luckey DW. Rhabdoid tumor of the kidney. A report of 111 cases from the national Wilms' tumor study pathology center. Am J Surg Pathol 1989;13:439-58.
26. Velasco ME, Brown JA, Kini J, Ruppert ES. Primary congenital rhabdoid tumor of the brain with neoplastic hydrancephaly. Child's Nerv Syst 1993;9:185-90.
27. Chou SM, Anderson JS. Primitive CNS malignant rhabdoid tumor (MRT): report of two cases and review of literature. Clin Neuropathol 1991;10:1-10.